

Modeling, simulation and implementation of imaging system for detection of hidden objects

Triveni Keskar^{1,2*}, Vijay R. Dahake¹, and Anuj Bhatnagar²

¹Department of Electronics and Telecommunication, Ramrao Adik Institute of Technology, Navi Mumbai, India

²Society for Applied Microwave Electronics Engineering and Research, IIT Bombay, Powai, India

* Email: trivenikeskar@gmail.com

(Received April 10, 2017)

Abstract: The proliferation of applicability of extremely high frequency band close to Terahertz frequencies for its signature characteristics such as reflection from metals, low loss transmission from non-polar dielectrics and specific absorption for wide range of liquids and drugs has been the interest behind this paper. We have modeled the system at 110 GHz to obtain simulation results justifying the system design. We have presented a practical implementation with 89.4 GHz IMPATT diode source for a small area TeraSense camera detector (4.5 cm × 4.5 cm) and an XY direction moving stage controlled by Holmarc MicroMotion platform for capturing raster scan imaging of large objects based on the results. We also have tried to make the result more intuitive to the user using edge detection and intensity analysis in image processing domain. We are able to detect non-invasively, an object within 34 cm × 22 cm area, in 4 minutes, which has been hidden under or inside a 4 mm thick cardboard or clothing covering.

Keywords: TracePro, MATLAB image processing, Symbolic math and GUI toolbox, Holmarc Micro Motion, TeraSense IMPATT diode.

doi: [10.11906/TST.062-070.2017.06.04](https://doi.org/10.11906/TST.062-070.2017.06.04)

1. Introduction

The rapid, non-destructive, non-invasive characterization and imaging of objects and defects in uniform materials or under coated surfaces has been of interest from the perspective of a wide range of application industries. The radiation at 110 GHz emulates characteristics of Terahertz Extremely High Frequency. Non-ionizing radiation and transparency to non-metallic-non-polar dielectrics highlights the applicability of this frequency band. It is highly reflective when obstructed by metals and has absorption signatures whilst passing through most liquids and explosives.

Presented in this paper is a green, low power, human friendly imaging system that will be very useful in security scanning, product composition and quality checking. Modeling a small area detector for large object detection through optically opaque layer, analysis of scanned images for providing a guiding output to an untrained user and edge detection are our key objectives achieved. We are able to establish that a metallic or liquid object can be detected through a 4 mm thick box made of plastic, paper, wool or acrylic.

A. Penetration depth of THz radiation

Penetration Depth defined as the depth at which the intensity of the radiation inside the material falls to $1/e$ of its original value beneath the surface. An electromagnetic radiation incident on a surface is lost in mainly three ways: reflection, absorption and transmission. Depending on the nature of the material, the electromagnetic field might travel very far into the material, or may die out very quickly. This phenomenon, dependent upon the frequency of incident radiation, can be quantified in terms of the equation of penetration depth as follows:

$$\delta = \sqrt{\frac{2}{\omega \mu \sigma}}$$

where, ω is the angular frequency for the radiation given by $2\pi f$, and $\mu \sigma$ is the product of permeability and conductivity specific to material. We have chosen three materials convenient to our project's scope, for modeling δ for Terahertz radiation from 100 GHz to 10 THz.

B. Chosen Specimen Materials

- (1) Teflon (dc conductivity 10^{-25} to 10^{-23} and permeability 1.2567×10^{-6} , transparent)
- (2) Water (dc conductivity 5×10^{-4} and permeability 1.256627×10^{-6} , absorption in liquids)
- (3) Iron (dc conductivity 1.00×10^7 and permeability 6.3×10^{-3} , reflection in liquids)

Thus, conductivity-productivity product for Teflon = 1.2567×10^{-31} , Water = 6.283135×10^{-10} and for iron it is 6.3×10^4 . We have deliberately created the plot in order to view all these material specific characteristics in question.

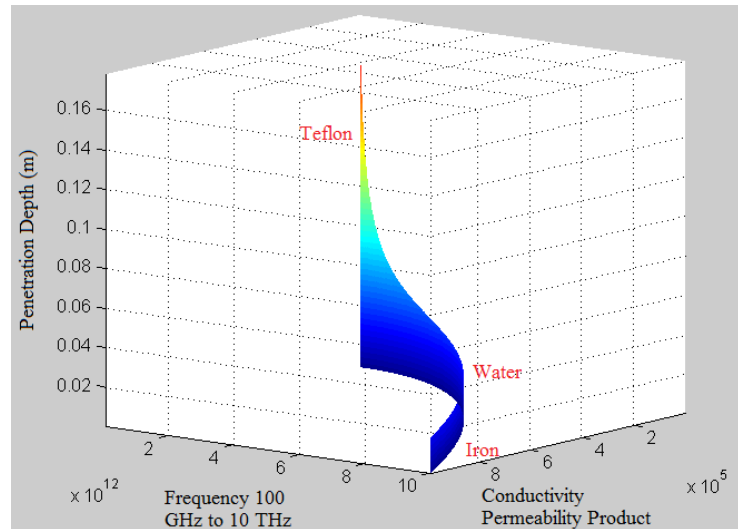


Fig. 1 Penetration depth for Teflon, Water and Iron over THz band

Teflon, being closest to the origin of this mesh plot, shows very high order of transmission for THz frequencies. To view these characteristics, we have plotted the calculated penetration depth separately for each isolated material as shown in the figure below:

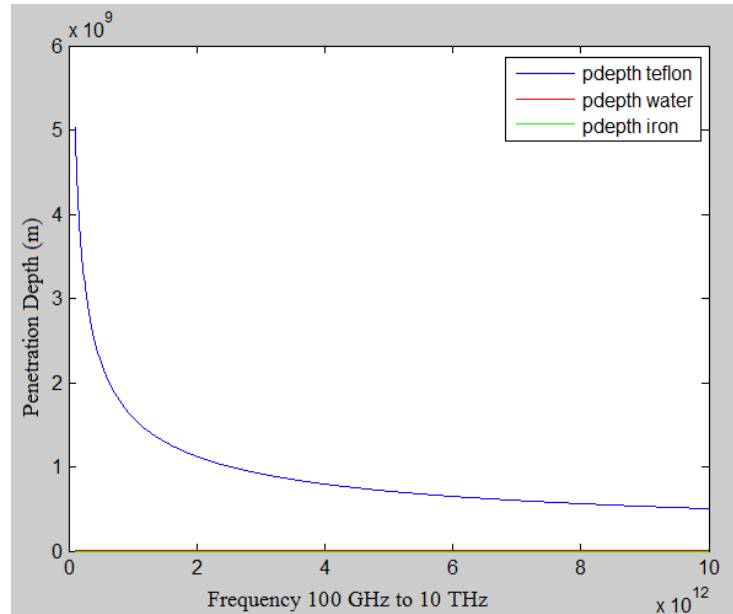


Fig.2 Penetration depth for isolated materials in THz band

2. Modeling of THz imaging system with raytrace simulation

The motivation behind this model is to be able to detect a metallic or liquid object inside a non-polar dielectric covering like plastic, clothing, box of cardboard, etc. We first begin with explanation of each component in detail and then proceed towards the appropriate distances for each object placement and the working of the simulation with irradiance map, after tracing the rays for our system.

A. Component description

The Terahertz model comprises of source at the origin of three axes. We have modeled the system along Z axis, since our stage is modeled in XY axes plane. In the model, we have proposed the distance between source and detector to be 70 cm, keeping the obstacles such as acrylic sheet at 40 cm, water object at 50 cm and the metallic gold surface at 60 cm. In practical implementation though, we have decided that these distances will be about half of the proposed ones, in order to avoid losses in scattering, more popularly known as path loss, which is directly proportional to the distance between the source and the detector.

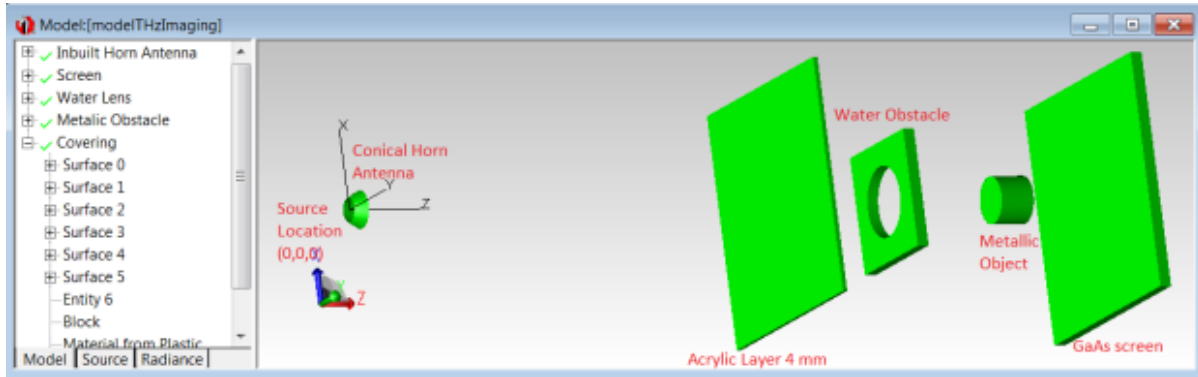


Fig. 3 THz Imaging Model along Z axis

(1) *Source*

We have chosen a grid source with annular grid boundary and circular grid pattern identical to the radiation pattern of TeraSense IMPATT diode [4]. Total flux of this source is 1 Watt and it has a uniform special-angular profile divergent from the focal point, with 271 rays for each wavelength nearby spaced for 110 GHz , 2.2727 mm , all possessing horizontal linear polarization. We have added a conical reflector, to reproduce the effect of horn antenna with divergence angle 18° .

(2) *Detector*

We have chosen as per our TeraSense camera detector with high speed electromagnetic radiation detection functionality [6], a GaAs substrate screen, with dimensions comparable to the screen-source distance for best understanding ($20\text{ cm} \times 20\text{ cm}$). Transmission spectroscopy is the basis behind the detection methodology, where captured normalized intensity pattern gets translated as RGB images at the software.

(3) *Obstacle 1: acrylic covering*

We have added an acrylic covering, where the penetration depth of radiation at 2.2727 mm , is quite high, giving absorption as good as 0 in the TracePro model for 4 mm thick layer.

(4) *Obstacle 2: water absorptive object*

We have added a lens object made of water, from liquids catalogue in TracePro model having auto-generated absorption ratio 8.19444 and transmission ratio $2.58233\text{e-}36$.

(5) *Obstacle 3: gold reflective surfaces*

We have chosen the IR Gold surface property for the metallic primitive block with the data table for wavelength 2.2727 mm showing absorbance coefficient 0.01 and reflection coefficient

0.989855011712889, which leaves approximately zero transmission through the metallic obstacle indicating a very low intensity spot at the screen behind it. However, we have purposefully kept the length of the materials nearby wavelength of the source, in order to also model the transmission based imaging system with diffracted rays, skewing their paths along the edges of the reflective surfaces, and reaching the screen through loss of intensity due to reflection and reorientation, taking a longer path to reach the screen than those of the other rays.

B. Simulation results

The rays from source originate at the focal point of the conical horn antenna, as a set of 271 rays per wavelength. The total flux radiated from the source undergoes expected changes as stated before and provides the results as below:

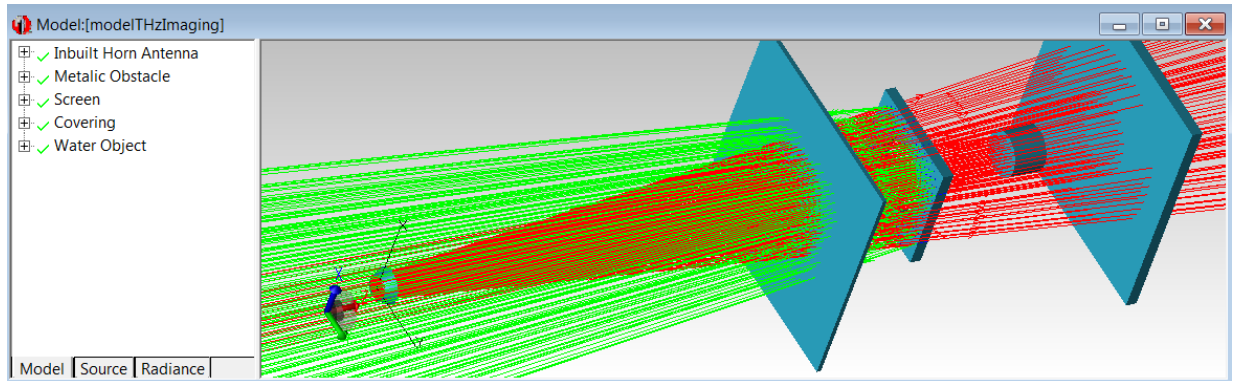


Fig. 4 THz Imaging Simulation for acrylic sheet thickness (a) 3 mm, (b) 3.5 mm, (c) 3.95 mm and (d) 4 mm

C. Irradiance map

The irradiance map is a map of flux per unit area portrayed in normalized intensity form for the surface of our choice. For demonstration purpose, we have chosen the screen's frontal face (directly opposed to the source) to view the irradiance of the source, whilst it reaches the screen past all the obstacles in between.

The rays have been traced only along the points where there was a transparent obstacle such as acrylic or paper in between. For the given diagram, there is no ray traced at the surface boundaries of metallic object or the water object, which ensures the correctness of our model. The beam profile adjacent to the irradiance map shows the intensity values represented as colours in previous plot on Y-axis.

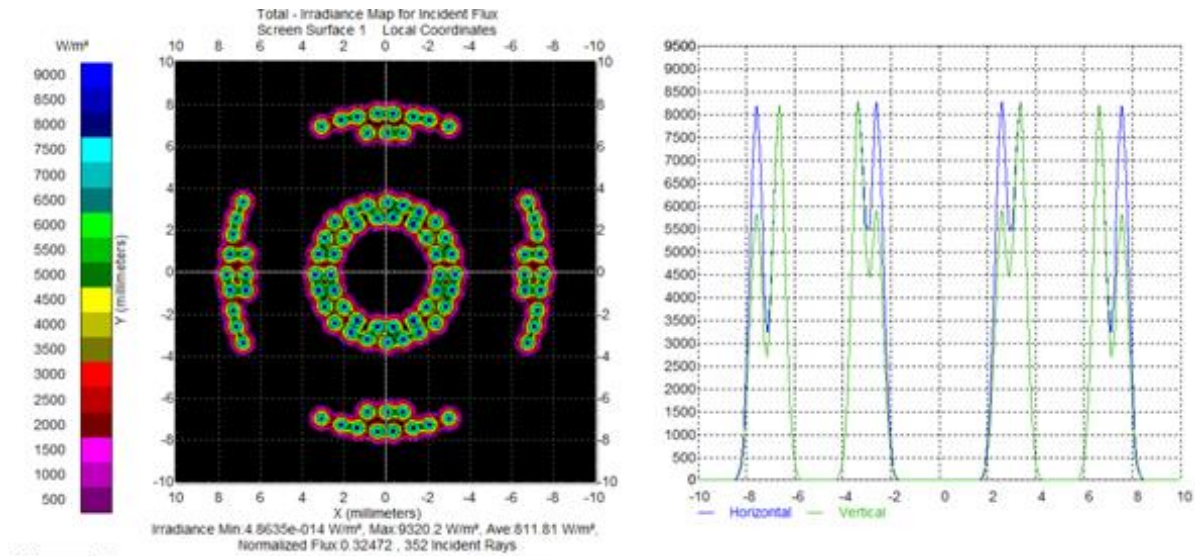


Fig. 5 Irradiance Map with Normalized rainbow colour scheme

3. Practical implementation

The only difference in practical implementation seems to be that the object will be much larger than the irradiance coverage of the source and screen widths. Thus, we are inclined towards using a movable XY stage which helps in translating the object under surveillance in a raster scanning motion [5] whilst the rest of the system is kept at the same position along Z axis. We go on taking a video of the obtained image frames throughout the scan and choose appropriate image frames arranged to form holistic $34\text{ cm} \times 22\text{ cm}$ stage image as presented in paper [5].

We have implemented MATLAB based algorithm for this purpose. Borrowing the results from our published work, we are presenting the intensity image of objects placed on the Holmarc MicroMotion Stage.

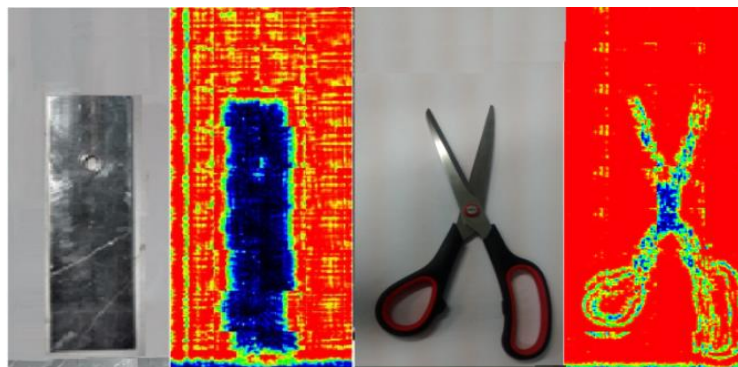


Fig. 6 Stitched intensity images of plate and scissor objects [5]

The idea is to perform image processing toolbox operations from MATLAB for analysis of these normalized intensity images and present the user with suggestive information.

4. Result representation

We have also added another image processing based result analysis, wherein, we try to calculate how much part of the stage is covered by low intensity if we were using a large detector which could process the whole object at once. Then, we predict the size of the real object from the pixel based stitched full image. For this purpose, we have developed the following algorithm:

- 1) Convert the image to binary (0 for black and 1 for white), keeping threshold at 0.05 calculated by 'grayscale' function of MATLAB useful for conversion of RGB image into binary.
- 2) Compute size of the image and value of (x, y) for the last pixel.
- 3) Begin reading pixel values starting from pixel (i, j) = (1,1) towards the right in x direction, with a for loop.
- 4) As the variable i reaches x, begin incrementing j in another for loop inside which the loop in 3 would be nested.
- 5) If the pixel value is 0 at i_0 and j_0 , save the $first_{point}$ as (i_0, j_0)
- 6) Now begin from end point and travel towards the left, negative direction for loops and follow procedure in 4 and 5, to determine end_{point} as (i_{end}, j_{end})
- 7) Draw a rectangle over the image object with starting point at (i_0, j_0) and end point at (i_{end}, j_{end})
- 8) Compute the x_{length} as $i_{end} - i_0$ and y_{length} as $j_{end} - j_0$ and find out the proportional values of real object using the following equations:

$$real(X_{length}) = length_{stage} * \frac{x_{length}}{x}, real(y_{length}) = width_{stage} \frac{y_{length}}{y}$$

- 9) Count the number of pixels with 0's as $count_{dark}$ and those with 1's as $count_{white}$. Calculate the percentage of low intensity area by the following equation:

$$percentage_{dark} = \frac{count_{dark}}{(count_{dark} + count_{white})}$$

- 10) Display the result for $percentage_{dark}$, $real(X_{length})$ and $real(y_{length})$.

At the end of implementation of this algorithm, we generate the results in a form which is not only easy to handle for a newbie over the system, regardless of the complexity of the object, but also error reduced than the systems where alert human lookout is mandatory. The GUI based result shown for the above mentioned plate object is as follows:

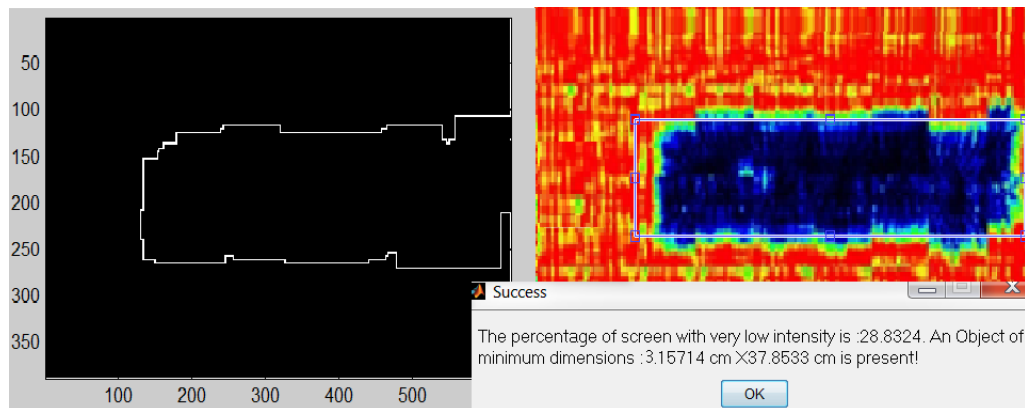


Fig. 7 THz imaging results for a metallic plate object after improvements

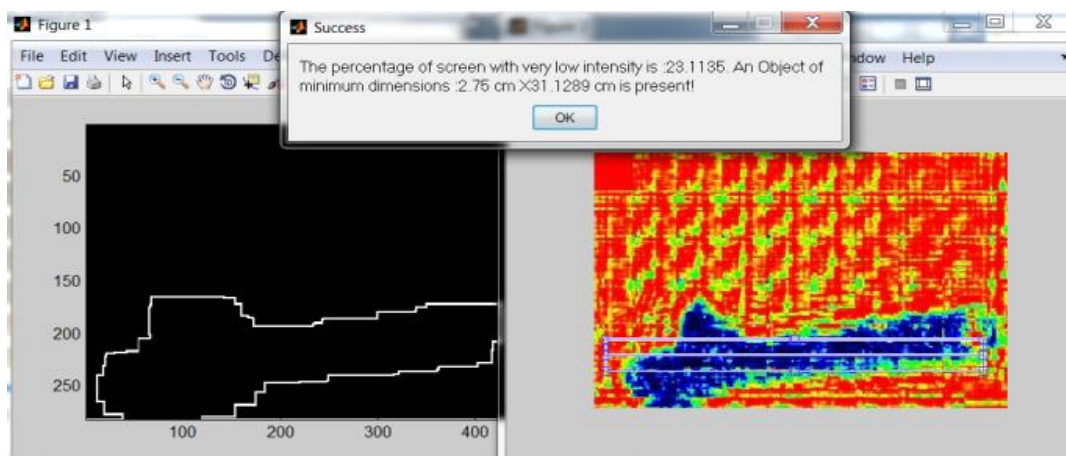


Fig. 8 GUI based result for metallic plier object detecting lost intensity area

Based on the percentage amount of intensity lost in the stage area, and its predicted location, it is predictable if there could be a suspicious object hidden inside, say, a bag of cloth or a box of paper.

5. Conclusion

With the modeling and simulation of Terahertz frequency imaging system components, we are able to quantify the total absorption, reflection and transmission of ray flux when the radiation passes through most of the liquids, non-polar dielectrics and metals. In comparison, practical intensity images at detector conform to the observed irradiation map pattern, thus making it possible to detect the shape of an object.

The narrative about the modeling and simulation presents with a more defined need for a large area detector in order to accomplish large object detection. But, as the detectors in this area range are quite costly, we decide to use a small TeraSense camera detector recording a scanning video,

only with a movable Holmarc stage to carry the object in XY direction, such that whole stage gets covered within 4 *minutes*. With image stitching, enhancement and edge detection algorithms, we have been able to successfully deliver a threat evaluated message to an untrained supervisor of the scanning system. In addition to the low error rate, this system is also healthy, non-invasive and green, as it makes no harmful ionizing radiation.

Acknowledgements

The authors would like to express their gratitude towards two immensely cooperative institutions Ramrao Adik Institute of Technology, affiliated to Mumbai University and Society for Applied Microwave Electronics Engineering Research, IIT Bombay (Department of Electronics Information Technology Ministry Of Communications Information Technology, Govt. of India) for providing with an inclusive, encouraging environment. Special thanks to our colleague Kshitij Mittholiya, for his active timely contribution in project and peer reviews were a pacemaker for us.

References

- [1] Basil A. M., Kshitij Mittholiya, Archana Hegde, et al. "Development of terahertz imaging system". *Journal of Instrumentation Society of India*, 45, 2, 30 June (2015).
- [2] Paul R. Karmel, Gabriel D. Colef, and Raymond L. Camisa. "Introduction to Electromagnetic and Microwave Engineering". *John Wiley & Sons*, 05 Jan (1998).
- [3] Somenath Ghatak, Ajit Kumar Meikap, of Physics, Manika Sinha, et al. "Electrical Conductivity, Magnetoconductivity and Dielectric Behaviour of (Mg,Ni)-Ferrite below Room Temperature". *National Institute of Technology, Deemed University, Durgapur, India, Department of Physics, University of Burdwan, Burdwan, India, Materials Sciences and Applications*, 2010, 1, 177-186. doi:10.4236/msa.2010.14028, 9 October (2010).
- [4] Wikipedia databases electrical conductivity, permeability and TeraSense website.
- [5] Triveni Keskar, Vijay R. Dahake. Department of Electronics and Telecommunication Engineering, Ramrao Adik Institute of Technology, Navi Mumbai, Kshitij Mittholiya, Archana Hegde, Basil A. M., Anuj Bhatnagar, Department of Photonics, Society of Applied Microwave Electronics Engineering and Research (SAMEER), Mumbai, "Development of MATLAB Based Image Stitching Tools for Detection of Hidden Objects at 89 GHz". *Advances in Optical Sciences and Technology*, Springer proceedings, 2017 (In publication).
- [6] Kukushkin, I. and Muravev, V. and Tsydynzhapov, G. and Fortunatov, A.. "High-speed giga-terahertz imaging device and method". *US Patent App.* 13/336,912, 27 June (2013)